A localization transition underlies the mode-coupling crossover of glasses

May 20, 2019

Contents

1 Analysis

Workflow and data analysis for "A localization transition underlies the mode-coupling crossover of glasses".

To quickly reproduce the analysis and check the results, use the convenience script `make` at the root of the data set

```
./make backup
./make clean
./make setup
./make analysis
./make check
```

Alternatively, execute the setup and analysis scripts individually from the terminal or follow the workflow described in this document.

The first level scripts (`src/tangle/analysis_1_*`) compute the following properties for each model:

- mobility edge and fractions of unstable modes
- average participation ratios as a function of eigenvalue
- mobility edge
- fractions of delocalized and localized unstable modes

Once the first level scripts have been executed, the second level scripts (`src/tangle/analysis_2_*`) compute the following:

- spectrum of unstable modes
- threshold energy
- level spacing statistics
- localization temperatures

There is no dependency between scripts of a given level. It is recommended to execute the scripts within the python virtual environment created by the `src/tangle/setup.sh` script.

1.1 Setup

The analysis scripts require the following python packages:

- `numpy` (1.16.3)
- `argh` (0.26.2)
- `atooms` (1.9.1)

We also require `gnuplot` (4.6.4 or higher) for a couple of fits.

The analysis scripts have been tested with both python 2.7 and 3.5.

Install all needed python packages in a python virtual environment (`env/`). This step is not strictly required if these packages are already installed system-wide.

```
# Require pip
if [[ ! -x $(command -v pip) ]] ; then
    echo The python package installer is required.
    echo Please install it with the following commands:
    echo   curl https://bootstrap.pypa.io/get-pip.py -o get-pip.py
    echo   python get-pip.py
    exit 1
fi
# Require virtualenv
if [[ ! -x $(command -v virtualenv) ]] ; then
    pip install --user virtualenv || exit 1
    export PATH=$PATH:$HOME/.local/bin
fi
# Require gnuplot
if [[ ! -x $(command -v gnuplot) ]] ; then
```

```
    echo Gnuplot is not installed.
    echo The setup will proceed, but it is recommended
    echo to install gnuplot via your software package manager
fi
# We freeze minor versions but accept bug fix updates
virtualenv -p python3 env
. env/bin/activate
pip install --upgrade numpy~=1.16.3
pip install --upgrade argh~=0.26.2
pip install --upgrade atooms~=1.9.1
deactivate
```

The convenience `make` script allows for batch execution of setup, analysis and gnuplot scripts. The `all` target reproduces the analysis and checks the results against a backup of the original dataset.

1.2 Reference MCT temperatures

Obtained from power law fits to dynamic data (literature data).

```
# This file can be sourced by gnuplot, bash, python
T_ss=0.20
T_karma=0.288
T_poly18=0.493
T_poly12=0.104
T_ntw=0.31
```

1.3 Mobility edge and fraction of modes

We determine the mobility edge λ_e using the finite-size scaling approach of Clapa, Kottos and Starr, JCP 2012. We look for the intersection of the scaled participation ratio $P(\lambda, L)/L$, for several linear system sizes L. Modes with eigenvalue $\lambda < \lambda_e$ are localized, those with $\lambda_e < \lambda_e < 0^-$. The inflection modes of quasi-stationary points ($|\lambda| \sim 10^{-4}$) is removed from the analysis.

1.3.1 Soft spheres

50-50 soft sphere mixture of Bernu et al.

```
echo "--------------------"
echo "Analyze soft spheres"
echo "--------------------"
```

Collect the participation ratio data.

```
echo "Collect participation ratio"
for N in 500 1000 2000 ; do
    for T in 0.2000 0.2207 0.2461 0.2783 0.3200 0.3764 0.4571 ; do
        dw=0.6 dw_true=2.0 inpfile=analysis/ss/N${N}/T${T}/modes_unstable.xyz src/tangle/
            localization_xyz.sh #2>/dev/null
    done
done
```

Detect the mobility edge programmatically. We must set a lower cut off on the eigenvalue that removes the noisy part of the data at large negative eigenvalues.

```
{
echo "# title: mobility edge lambda_e as a function of temperature T"
echo "# columns: T, lambda_e, P(lambda_e), error on lambda_e, missing intersections"
for T in 0.2000 0.2207 0.2461 0.2783 0.3200 0.3764 0.4571 ; do
    xmin=-10
    [ $T == 0.2000 ] && xmin=-3
    [ $T == 0.2207 ] && xmin=-4
    [ $T == 0.2461 ] && xmin=-6
    [ $T == 0.3200 ] && xmin=-10
```

```
    [ $T == 0.3764 ] && xmin=-15
    [ $T == 0.4571 ] && xmin=-18
    echo $T $(python src/mobility_edge.py --xmin $xmin analysis/ss/N*/T${T}/pratio_unstable.txt)
done
} | tee analysis/ss/mobility_edge.txt
```

Extract the fractions of modes.

```
echo "Extract fractions of unstable modes"
export dirout=analysis/ss
export mobility_edge=$dirout/mobility_edge.txt
N=500 src/tangle/localization_fraction_xyz.sh
N=1000 src/tangle/localization_fraction_xyz.sh
N=2000 src/tangle/localization_fraction_xyz.sh
```

1.3.2 Ternary mixture

Ternary mixture of Karmakar et al.

```
echo "-----------------------"
echo "Analyze ternary mixture"
echo "-----------------------"
```

Collect the participation ratio data.

```
echo "Collect participation ratio"
for N in 250 500 1000 ; do
     for T in 0.27 0.28 0.29 0.30 0.32 0.35 0.45; do
         dw=1.5 dw_true=3.0 inpfile=analysis/karma/N${N}/T${T}/modes_unstable.xyz src/tangle/
             localization_xyz.sh
    done
done
for N in 3000 ; do
     for T in 0.29 0.30 0.32 0.35 0.45; do
         dw=1.5 dw_true=3.0 inpfile=analysis/karma/N${N}/T${T}/modes_unstable.xyz src/tangle/
             localization_xyz.sh
    done
done
```

Detect the mobility edge programmatically.

```
{
echo "# title: mobility edge lambda_e as a function of temperature T"
echo "# columns: T, lambda_e, P(lambda_e), error on lambda_e, missing intersections"
for T in 0.27 0.28 0.29 0.30 0.32 0.35 0.45 ; do
    echo $T $(python src/mobility_edge.py --xmin -15 analysis/karma/N*/T${T}/pratio_unstable.txt)
done
} | tee analysis/karma/mobility_edge.txt
```

Extract the fractions of unstable modes.

```
echo "Extract fractions of unstable modes"
export dirout=analysis/karma
export mobility_edge=analysis/karma/mobility_edge.txt
N=250 src/tangle/localization_fraction_xyz.sh
N=500 src/tangle/localization_fraction_xyz.sh
N=1000 src/tangle/localization_fraction_xyz.sh
```

1.3.3 Network liquid

Network liquid by Coslovich and Pastore

```
echo "----------------------"
echo "Analyze network liquid"
echo "----------------------"
```

Collect the participation ratio data.

```
echo "Collect participation ratio"
system=ntw
for N in 400 800 2000 ; do
    for T in 0.2900 0.3100 0.3397 0.3716 0.4120 ; do
      dw=1.0 inpfile=analysis/$system/N${N}/T${T}/modes_unstable.xyz src/tangle/localization_xyz.sh
          2>/dev/null
    done
done
```

Detect the mobility edge programmatically.

```
system=ntw
{
    echo "# title: mobility edge lambda_e as a function of temperature T"
    echo "# columns: T, lambda_e, P(lambda_e), error on lambda_e, missing intersections"
    for T in 0.2900 0.3100 0.3397 0.3716  0.4120 ; do
        xmin=-10
        [ $T == 0.2900 ] && xmin=-3
        [ $T == 0.3100 ] && xmin=-3
        [ $T == 0.3397 ] && xmin=-6
        [ $T == 0.4120 ] && xmin=-10
        echo $T $(python src/mobility_edge.py --xmin $xmin analysis/$system/N{400,800,2000}/T${T}/
            pratio_unstable.txt)
    done
} | tee analysis/$system/mobility_edge.txt
```

Extract the fractions of modes.

```
echo "Extract fractions of unstable modes"
system=ntw
export dirout=analysis/$system
export mobility_edge=$dirout/mobility_edge.txt
N=400 src/tangle/localization_fraction_xyz.sh
N=800 src/tangle/localization_fraction_xyz.sh
N=2000 src/tangle/localization_fraction_xyz.sh
```

1.3.4 Polydisperse n=18

Additive polydisperse soft sphere model with exponent n=18 (Ninarello et al. PRX 2017).

```
echo "------------------------"
echo "Analyze polydisperse 18"
echo "------------------------"
```

Collect the participation ratio data.

```
echo Collect participation ratio
for N in 250 500 1500 ; do
    for T in 0.330 0.350 0.390 0.432 0.471 0.517 0.586 0.682 ; do
        dw=2.0 inpfile=analysis/poly18/N${N}/T${T}/modes_unstable.xyz src/tangle/localization_xyz.sh
             2>/dev/null
    done
done
```

Detect the mobility edge programmatically.

```
system=poly18
{
    echo "# title: mobility edge lambda_e as a function of temperature T"
    echo "# columns: T, lambda_e, P(lambda_e), error on lambda_e, missing intersections"
    for T in 0.330 0.350 0.390 0.432 0.471 0.517 0.586 0.682 ; do
        xmin=-10
        [ $T == 0.330 ] && xmin=-4
        [ $T == 0.350 ] && xmin=-4
        [ $T == 0.390 ] && xmin=-4
        [ $T == 0.432 ] && xmin=-4
```

```
        [ $T == 0.471 ] && xmin=-4
        [ $T == 0.517 ] && xmin=-6
        [ $T == 0.586 ] && xmin=-10
        [ $T == 0.682 ] && xmin=-15
        echo $T $(python src/mobility_edge.py --xmin $xmin analysis/$system/N*/T${T}/pratio_unstable
            .txt)
    done
} | tee analysis/$system/mobility_edge.txt
```

Extract the fractions of modes.

```
echo "Extract fractions of unstable modes"
system=poly18
export dirout=analysis/$system
export mobility_edge=$dirout/mobility_edge.txt
N=250 src/tangle/localization_fraction_xyz.sh
N=500 src/tangle/localization_fraction_xyz.sh
N=1500 src/tangle/localization_fraction_xyz.sh
```

1.3.5 Polydisperse n=12

Non-additive polydisperse soft sphere model with exponent n=12 (Ninarello et al. PRX 2017).

```
echo "-----------------------"
echo "Analyze polydisperse 12"
echo "-----------------------"
```

Collect the participation ratio.

```
echo "Collect participation ratio"
for N in 250 500 1500 ; do
     for T in 0.062 0.075 0.092 0.110 0.120 0.150 ; do
         touch analysis/poly12/N${N}/T${T}/modes.nin
         dw=1.0 dw_true=2.0 inpfile=analysis/poly12/N${N}/T${T}/modes.nin src/tangle/
             localization_xyz.sh
     done
done
```

Get the mobility edge.

```
{
    echo "# title: mobility edge lambda_e as a function of temperature T"
    echo "# columns: T, lambda_e, P(lambda_e), error on lambda_e, missing intersections"
    for T in 0.062 0.075 0.092 0.110 0.120 0.150 ; do
        echo $T $(python src/mobility_edge.py --xmin -6 analysis/poly12/N*/T${T}/pratio_unstable.txt
            )
    done
} | tee analysis/poly12/mobility_edge.txt
```

Compute fraction of unstable modes.

```
echo "Extract fractions of unstable modes"
export file_base=modes.nin
export dirout=analysis/poly12
export mobility_edge=analysis/poly12/mobility_edge.txt
export Wcut=3e-9
N=250 src/tangle/localization_fraction_xyz.sh
N=500 src/tangle/localization_fraction_xyz.sh
N=1500 src/tangle/localization_fraction_xyz.sh
```

1.4 Vibrational density of states

We analyze the crossover between power law and exponential in the unstable portion of the spectrum $g(\lambda)$.

1.4.1 Ternary mixture

Compute the spectrum of the ternary mixture. Remove the spurious inflection mode around $|\lambda| \sim 10^{-4}$ in quasi-stationary modes.

```
echo "Vibrational density of states"
echo "-----------------------------"
for N in 250 500 1000 ; do
    for T in 0.27 0.28 0.29 0.30 0.32 0.35 0.45 ; do
        inpfile=analysis/karma/N${N}/T${T}/modes_unstable.xyz
        outfile=analysis/karma/N${N}/T${T}/vdos_unstable.txt
        {
            echo "# title: spectrum g(lambda) of the unstable modes with eigenvalue lambda"
            echo "# note: the inflection mode with |lambda|<1e-4 is removed from the analysis "
            echo "# columns: lambda, g(lambda)"
            awk "(NF>1) && (\$1<-1e-4){print \$1}" $inpfile | grep -v step | src/dist.py -c 0 -
        } > $outfile
    done
done
```

1.5 Level spacing statistics

We analyze the level spacing statistics and check the crossover between Wigner-Dyson and Poisson distributions.

1.5.1 Ternary mixture

We analyze the ternary mixture. The mobility edge at T=0.35 is around -4.9. We remove the modes around the edge (over a range ± 2), for which the functional form of the lavel spacing statistics has an intermediate character.

```
echo "Level spacing"
echo "-------------"
inpfile=analysis/karma/N3000/T0.35/modes_unstable.xyz
outdir=analysis/karma/N3000/T0.35/
python src/modes.py spacing --lambda-max -6.9                      $inpfile | src/dist.py -c 0 -b 30
    - > $outdir/spacing_localized_unstable.txt
python src/modes.py spacing --lambda-min -2.9 --lambda-max -0.0001 $inpfile | src/dist.py -c 0 -b 30
    - > $outdir/spacing_delocalized_unstable.txt
```

1.6 Energy threshold

We determine the energy threshold e_{th} from the vanishing of the fraction of delocalized modes. For the models in which the fraction becomes strictly zero at a finite T we can do it explicitly. For the soft spheres it is very close, so we must extrapolate. The network liquid has no energy threshold. Note: a more accurate approach would be fitting f_u vs. e_s, e.g. by the p-spin functional form, as we do to determine the localization transition temperature.

```
echo "Energy threshold"
echo "----------------"
echo 1.74 > analysis/ss/threshold_energy.txt  # for soft spheres we have to extrapolate because we
    do not cross it
awk '($6==0.0){print $3}' analysis/karma/N1000/fraction_localization.txt | sort -g | tail -n 1  >
    analysis/karma/threshold_energy.txt
awk '($6==0.0){print $3}' analysis/poly12/N1500/fraction_localization.txt | sort -g | tail -n 1 >
    analysis/poly12/threshold_energy.txt
awk '($6==0.0){print $3}' analysis/poly18/N1500/fraction_localization.txt | sort -g | tail -n 1 >
    analysis/poly18/threshold_energy.txt
```

1.7 Analysis as a function of energy

We gather saddles by energy across temperatures. We compute the fractions of modes for fixed e_s, Note that in order to properly build the $f_u(e_s)$ plot we should reweight the energies by the Boltzmann weight. This is not done here.

```
echo "Analysis as a function of energy"
echo "--------------------------------"
for N in 250 500 1000 ; do
    mkdir -p analysis/karma/N${N}/gather
    ./src/modes.py gather --fraction --fraction-output "analysis/karma/N${N}/gather/fraction.txt"
             --de 0.02 --lambda-cut 1e-4 analysis/karma/N${N}/T0.*/modes_unstable.xyz
    ./src/modes.py gather --fraction --fraction-output "analysis/karma/N${N}/gather/fraction_true.
        txt" --de 0.02 --only true-saddles analysis/karma/N${N}/T0.*/modes_unstable.xyz
done
```

1.8 Localization transition temperature

We determine the localization transition temperature from a linear fit of the mobility edge. Bash wrapper to the above gnuplot script

```
echo "Localization transition temperature"
echo "-----------------------------------"
gnuplot src/tangle/analysis_2_localization_temperature.gp
```

2 Plots

To produce all the figures

```
for f in plots/paper/[a-z]*.gp ; do
  gnuplot $f
done
```

The paper's figures have been produced using `gnuplot` 5.0.0.

2.1 Overview (Figure 1)

Overview on the main result: the geometric transition only applies to the fraction of delocalized unstable modes f_{ud}, which vanishes at a temperature close to the MCT temperature determined from fitting the dynamic data. The fraction of localized unstable modes f_{ud} is model-dependent.

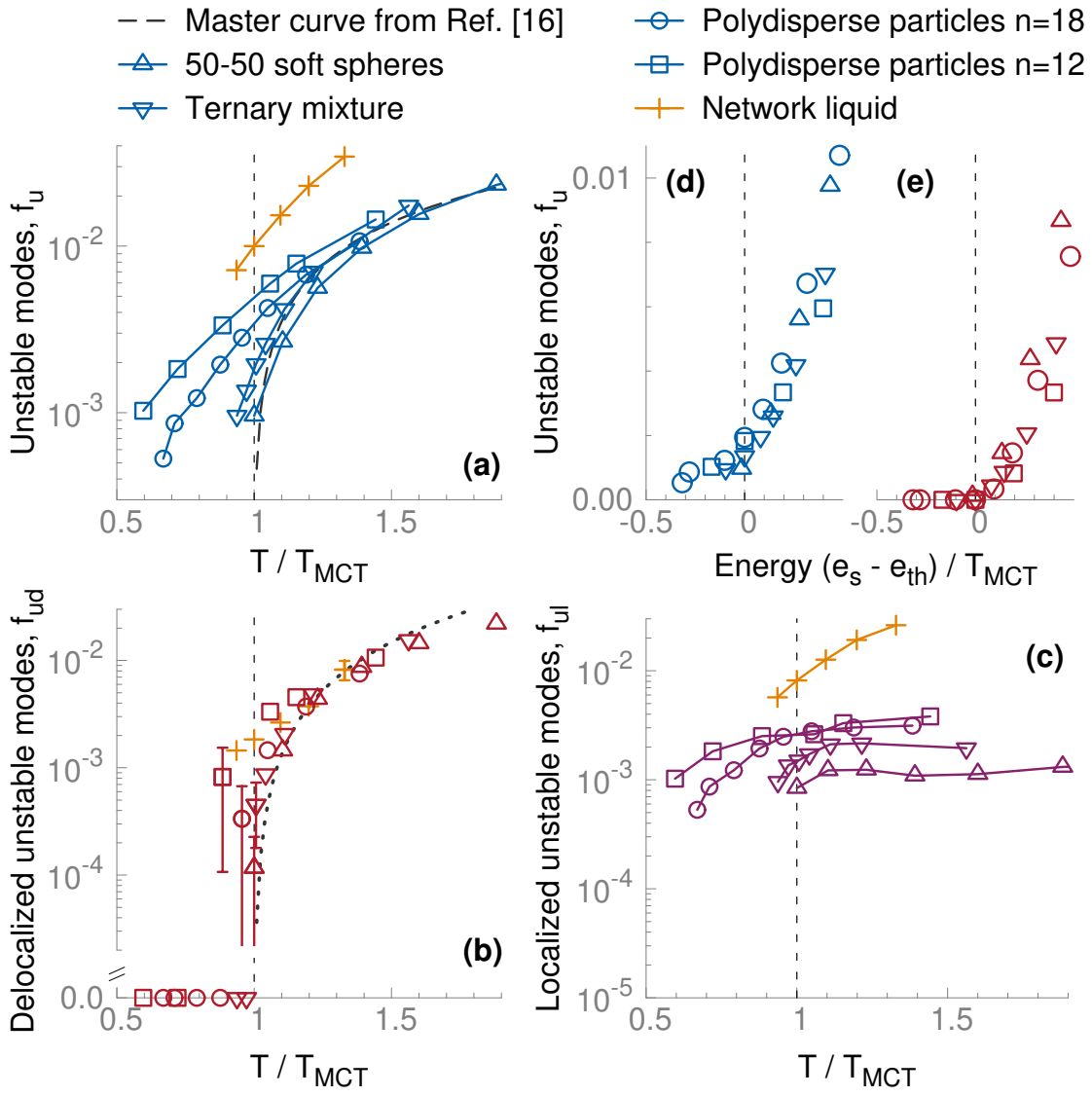

Figure 1: Fraction of unstable modes, delocalized unstable modes and localized unstable modes for all the studied models.

2.2 Mobility edge (Figure 2)

We illustrate the numerical determination of the mobility edge for the ternary mixture. The participation ratio of a mode α is defined as

$$P_\alpha = \left(\frac{1}{N} \sum_i (\vec{e}_i^{\,\alpha})^4 \right)^{-1}$$

where $\vec{e}_i^{\,\alpha}$ is the vector displacement of particle i in mode α. We then compute the average participation ratio $P(\lambda)$ of modes with (negative) eigenvalue λ. The mobility edge λ_e is identified by the fixed point of $P(\lambda, L)/L$ where L is the linear size of the system.

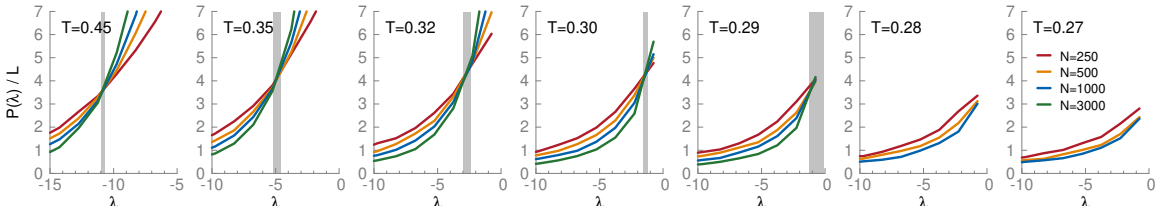

Figure 2: Scaled average participation ratio for the ternary mixture.

2.3 Localization transition from mobility edge (Figure 3)

We determine the localization transition temperature T_λ from the vanishing of the mobility edge λ_e. A least square fit provides a precise determination of the localization temperature.

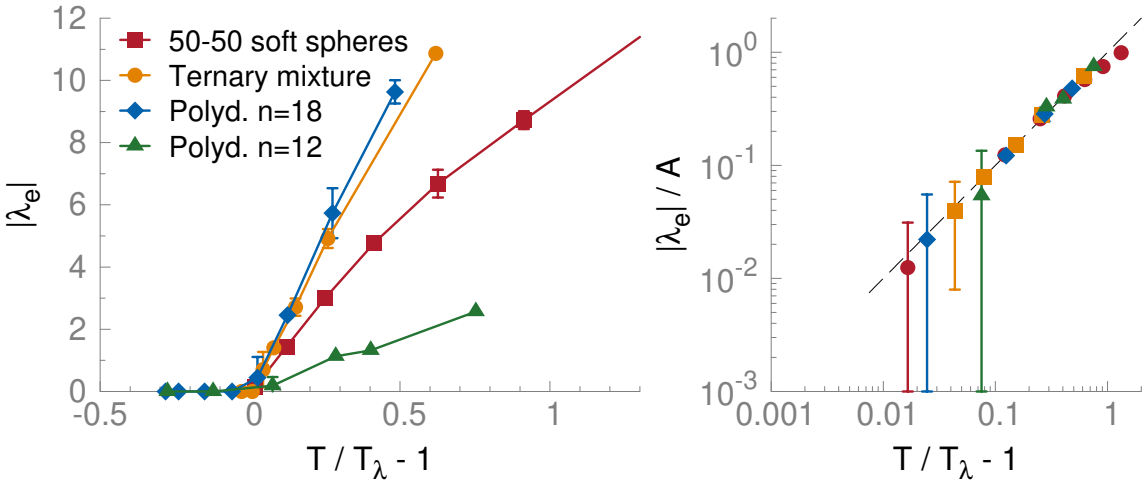

Figure 3: Temperature dependence of the mobility edge λ_e and localization transition temperature T_λ in all the studied models.

2.4 Vibrational density of states (Figure 4)

We look at the shape of the unstable spectrum $g(\lambda)$ of the dynamical matrix. Two distinct behaviors can be identified, associated to delocalized and localized modes, respectively. For small absolute eigenvalues (delocalized modes), the spectrum has a power law behavior

$$D(\lambda) = A(\lambda - \lambda_0)^\nu$$

This functional form is found in the mean-field p-spin model and is consistent with the β regime dynamics predicted by MCT.

For large absolute eigenvalues (localized modes), we expect an exponential tail

$$D(\lambda) = A \exp(-B\lambda)$$

We observe these two regimes above the MCT temperature. The crossover between the two regimes occur somewhat below the mobility edge. Below the MCT temperature, the spectrum is exponential.

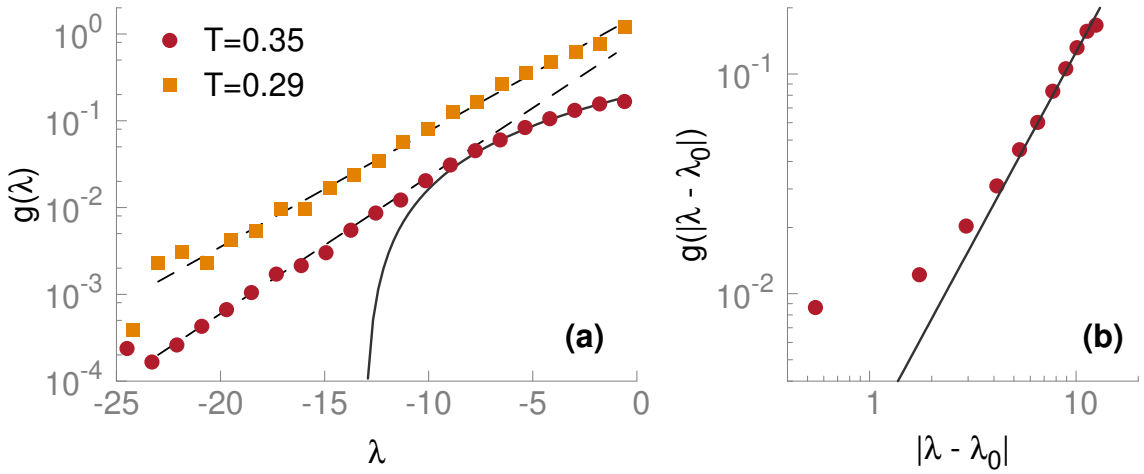

Figure 4: Spectrum of unstable modes $g(\lambda)$ for the ternary mixture.

2.5 Level spacing statistics (Figure 5)

We study the statistics of level spacings s. Above T_{MCT}, we can distinguish the two kinds of behaviors. For delocalized modes, the Wigner-Dyson distribution

$$P(s) = (\pi s/2) \exp(-\pi s^2/4)$$

works well, while for localized modes, the distribution is close to Poissonian

$$P(s) = \exp(-s)$$

We remove modes around the mobility edge, over a range of eigenvalues $\pm\delta = 2$, because these modes are known to have a mixed character. The choice $\delta = 1$ also gives good agreement with the two functional forms above.

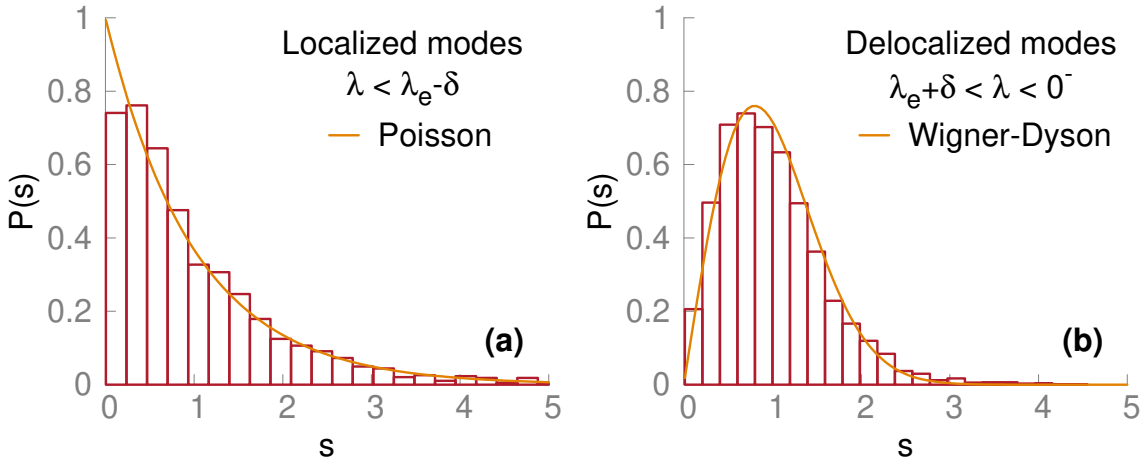

Figure 5: Distribution of level spacing for the ternary mixture.

2.6 Quasi-stationary points versus stationary points (Figures 6 – 8)

In this section we compare the statistical properties of quasi-stationary and stationary points for the ternary mixture. We focus on this model because it is the one for which we accumulated the largest statistics.

The geometric plot $e_s(f_u)$ shows results obtained separately for stationary points and for the bulk of the points obtained from minimizations of the mean square force W. Only minor discrepancies between the two sets of data are visible, the fraction of unstable modes being slightly smaller in stationary points at small e_s.

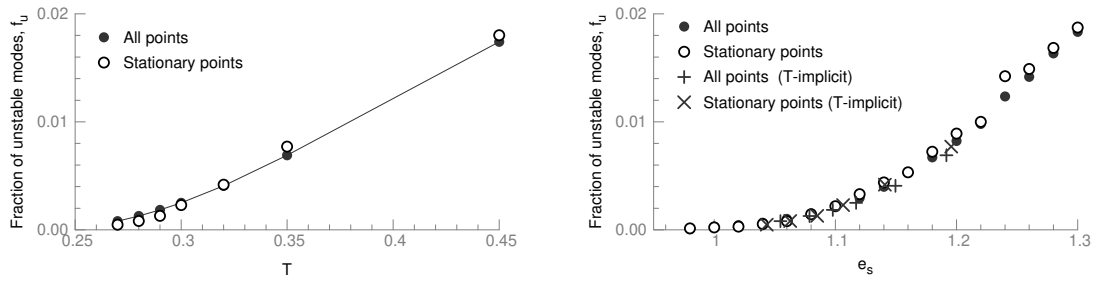

Figure 6: Geometric plot $e_s(f_u)$ for all the points and for stationary points in the ternary mixture.

We show the participation ratio $P(\lambda)$ of the unstable modes for all points obtained from all minimizations and for stationary points only. The two sets of data are fairly consistent with one another.

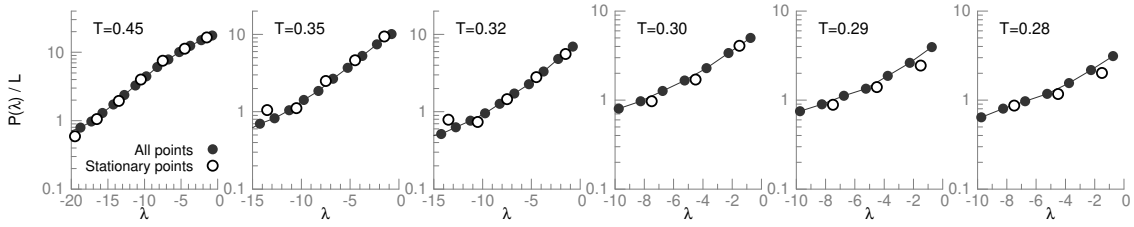

Figure 7: Scaled participation ratio for all the points and for stationary points in the ternary mixture.

We show the fraction of delocalized unstable modes for stationary points only, *i.e.* without quasi-stationary points. We use the mobility edge obtained from analysis of all W minimizations because the current statistics on the participation ratio is not sufficient to determine the mobility edge.

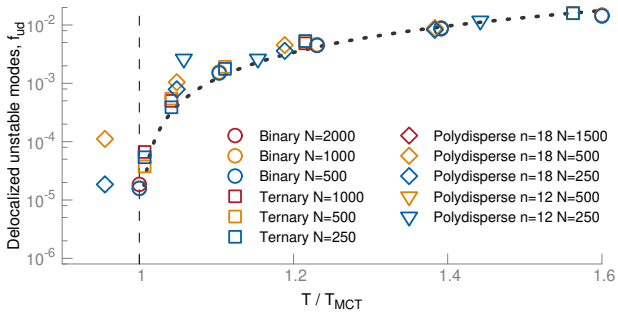

Figure 8: Fraction of delocalized modes for all the points and for stationary points in the ternary mixture.

3 Supplement

Supplementary information for "A localization transition underlies the mode-coupling crossover of glasses"

To produce all the figures in the supplement

```
for f in plots/si/[a-z]*.gp; do
    gnuplot $f
done
```

The supplement's figures have been produced using `gnuplot` 5.0.0.

3.1 Methods

We determined stationary and quasi-stationary points of the potential energy surface (PES) for systems of N point particles by minimizing the total squared force

$$W = \frac{1}{N}\sum_{i=1}^{N} |\vec{f}_i|^2 \tag{1}$$

where $\vec{f}_i$ is the force on particle i. Minimizations start from instantaneous configurations obtained from Monte Carlo or molecular dynamics simulations at a given number density $\rho = N/V$ and temperature T. For each configuration, we used the l-BFGS minimization algorithm [9] to minimize W. It is well-known that W minimizations locate *true* stationary points only rarely [11] and that the vast majority of points determined with this method are quasi-stationary points, at which there is precisely one inflection mode having a null zero eigenvalue [4]. In our minimizations, this inflection mode has a nearly zero eigenvalue whose norm $|\lambda|$ is typically between 10^{-6} and 10^{-4} (in the corresponding reduced units, see below) and which is clearly distinguishable from the lowest non-zero eigenvalue for the system sizes used in this work. The inflection mode was removed from the analysis, to avoid spurious $O(1/N)$ finite size effects when the fraction of unstable modes gets close to zero.

The stationary and quasi-stationary points can be distinguished from the corresponding value of W (in reduced units), which is low but non-zero for quasi-stationary points and zero within machine precision for true stationary points ($W \sim 10^{-14}$). In practice, we use a threshold of $\sim 10^{-10}$ to classify the two kinds of points for all models except for the polydisperse spheres with $n = 12$ (see below), for which a slightly higher threshold is used (3×10^{-9}) to account for a less strict convergence criterion on W minimizations. Previous studies showed that the statistical properties of quasi-stationary points and stationary points are practically indistinguishable above T_{MCT} [11].

3.2 50-50 Soft spheres

This is the historical 50:50 binary mixture introduced by Bernu *et al.* [1]. The pair interaction potential is

$$u_{\alpha\beta}(r) = \epsilon\left(\frac{\sigma_{\alpha\beta}}{r}\right)^{12} \tag{2}$$

where $\alpha, \beta = A, B$ are species indexes. The size ratio is $\frac{\sigma_{AA}}{\sigma_{BB}} = 1.2$ and the cross-interaction term is additive $\sigma_{AB} = (\sigma_{AA} + \sigma_{BB})/2$. The potential is cutoff and shifted at a distance $r_{cut} = \sqrt{3}\sigma_{AA}$ by adding a cubic term that ensures continuity of the potential up to the second derivative at r_{cut} [6, 5]. Energies and distances are expressed in units of ϵ and σ_{AA}, respectively. We used configurations from previous molecular dynamics simulations for N particles at a number density $\rho = N/V = 1$, with $N = 400, 800, 2000$ [2].

Table 1: Number of analyzed configurations for the 50-50 soft sphere mixture. The number in parenthesis indicates the corresponding number of true stationary points obtained.

–	$T = 0.2000$	$T = 0.2207$	$T = 0.2461$	$T = 0.2783$	$T = 0.3200$	$T = 0.3764$	$T = 0.4571$
$N = 500$	2800(24.1%)	3600(11.2%)	2000(12.0%)	800(15.8%)	800(17.5%)	2000(20.4%)	1000(19.5%)
$N = 1000$	3600(5.2%)	3600(2.3%)	800(3.1%)	800(7.0%)	800(9.4%)	800(9.4%)	400(7.2%)
$N = 2000$	1600(0.6%)	1600(0.0%)	800(0.6%)	800(3.0%)	800(4.8%)	800(4.2%)	400(5.0%)

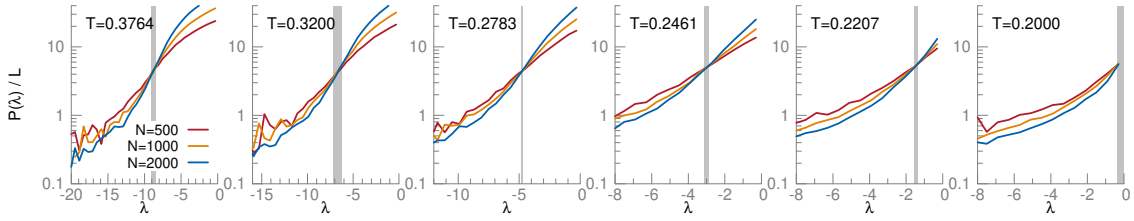

Figure 9: Averaged scaled participation ratio as a function of eigenvalue λ for the 50-50 soft sphere mixture. Vertical arrows mark the mobility edge λ_e at a given temperature. The width of the vertical bar is representative of the uncertainty on λ_e.

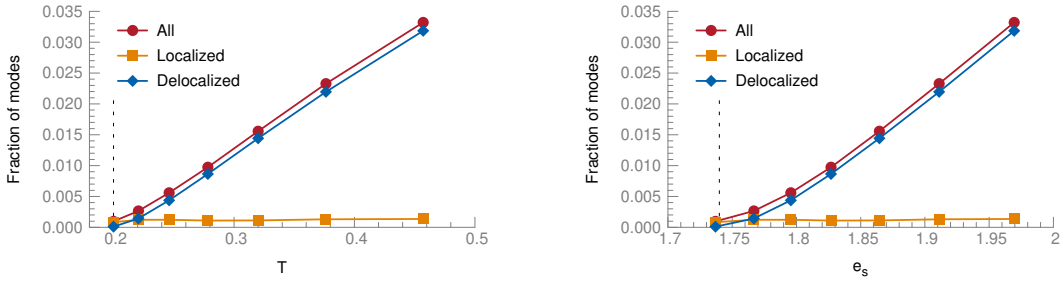

Figure 10: Fraction of unstable modes as a function of (a) temperature and (b) energy for the 50-50 soft sphere mixture ($N = 2000$). Vertical arrows in panel (a) and (b) mark the mode-coupling temperature T_{MCT} and the threshold energy e_{th}, respectively.

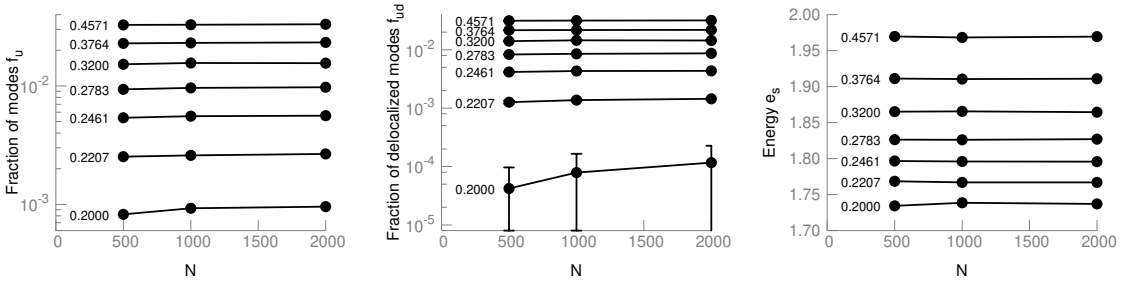

Figure 11: (a) Fraction of unstable modes, (b) fraction of delocalized unstable modes and (c) energy of stationary points as a function of the number of particles N for the 50-50 soft sphere mixture

3.3 Ternary mixture

The ternary mixture model studied in this work was introduced by Gutierrez *et al.* in Ref. [7]. The interaction potential is given by inverse power laws with an exponent 12, plus additional terms that ensure continuity of the derivatives at the cutoff:

$$u_{\alpha\beta}(r) = \left(\frac{\sigma_{\alpha\beta}}{r}\right)^{12} + c_4\left(\frac{\sigma_{\alpha\beta}}{r}\right)^{-4} + c_2\left(\frac{\sigma_{\alpha\beta}}{r}\right)^{-2} + c_0 \tag{3}$$

where $\alpha, \beta = A, B, C$ The expressions for c_0, c_2, and c_4 are given in [8]. The size ratio between two species is $\frac{\sigma_{AA}}{\sigma_{BB}} = \frac{\sigma_{BB}}{\sigma_{CC}} = 1.25$ and the chemical compositions are $x_A = 0.55$, $x_B = 0.30$, and $x_c = 0.15$. The potential is cut off at a distance $r_{cut} = 1.25\sigma_{\alpha\beta}$. We performed swap Monte Carlo simulations for $N = 250, 500, 1500, 3000$ particles at a number density $\rho = 1.1$. We used 80% of displacement moves over cubes of side $0.14\sigma_{AA}$ and 20% of swap moves [10]. To save computational time, we never attempted to exchange the identity of species A and C. We note that this model liquid can be equilibrated with swap Monte Carlo below the mode-coupling temperature $T_{MCT} = 0.29$ [10]. However, because of its crystallization tendency at low temperature, we could

not simulate the metastable liquid with $N = 1500$ particles for $T < 0.27$ and the one with $N = 3000$ particles for $T < 0.28$. Energies and distances are expressed in units of ϵ and σ_{AA}, respectively.

Table 2: Number of analyzed configurations for the ternary mixture. The number in parenthesis indicates the corresponding number of true stationary points obtained.

–	$T = 0.27$	$T = 0.28$	$T = 0.29$	$T = 0.30$	$T = 0.32$	$T = 0.35$	$T = 0.45$
$N = 250$	5200(32.0%)	5200(22.6%)	5200(14.7%)	4000(10.8%)	4000(7.0%)	4000(6.6%)	4000(8.8%)
$N = 500$	4200(11.0%)	4086(6.1%)	4000(2.6%)	3400(1.5%)	3400(0.7%)	3400(1.2%)	3400(3.1%)
$N = 1000$	4400(1.2%)	4400(0.3%)	4400(0.1%)	4000(0.1%)	4000(0.0%)	4000(0.1%)	4000(0.8%)
$N = 3000$	0()	0()	450(0.0%)	450(0.0%)	450(0.0%)	180(0.0%)	90(0.0%)

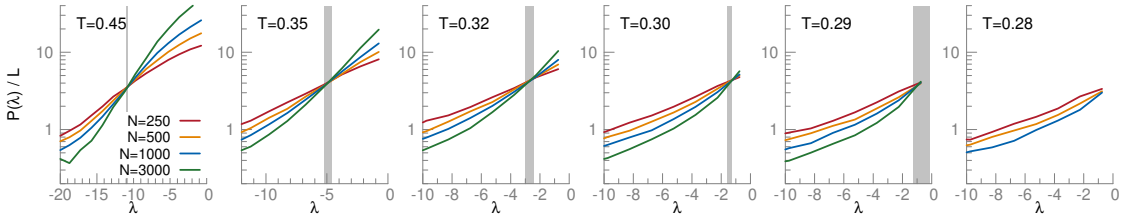

Figure 12: Averaged scaled participation ratio as a function of eigenvalue λ for the ternary mixture. Vertical arrows mark the mobility edge λ_e at a given temperature. The width of the vertical bar is representative of the uncertainty on λ_e.

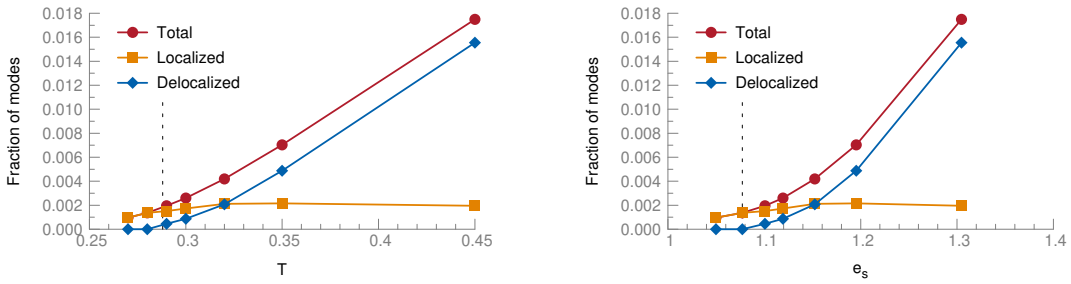

Figure 13: Fraction of unstable modes as a function of (a) temperature and (b) energy for the ternary mixture ($N = 1000$). Vertical arrows in panel (a) and (b) mark the mode-coupling temperature T_{MCT} and the threshold energy e_{th}, respectively.

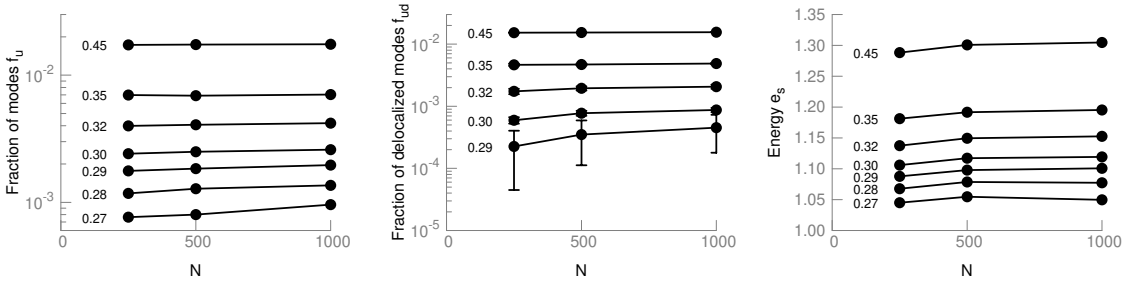

Figure 14: (a) Fraction of unstable modes, (b) fraction of delocalized unstable modes and (c) energy of stationary points as a function of the number of particles N for the ternary mixture

3.4 Network liquid

The network liquid model is a simple binary mixture that mimics the structure and dynamics of silica [3]. The interaction potential between unlike species ($\alpha \neq \beta$) is of the Lennard-Jones type

$$u_{\alpha\beta}(r) = 4\epsilon_{\alpha\beta}\left[\left(\frac{\sigma_{\alpha\beta}}{r}\right)^{12} - \left(\frac{\sigma_{\alpha\beta}}{r}\right)^{6}\right] \tag{4}$$

while the one between equal species is a simple inverse power

$$u_{\alpha\alpha} = \epsilon_{12}(\sigma/r)^{12} \tag{5}$$

Energies and distances are expressed in units of ϵ_{AA} and σ_{AA}, respectively. The remaining interaction parameters are $\epsilon_{AB} = 6$, $\sigma_{AB} = 0.49$, $\sigma_{BB} = 0.85$, $\epsilon_{BB} = 1$ The potential is cut off smoothly at r_{cut} by adding a cubic term that ensures continuity of the second derivative at the cut off distance r_{cut}, as for the soft sphere mixture [5]. The resulting cut-off distances are 2.07692, 1.39081, 1.76538 for $A-A$, $A-B$ and $B-B$ interactions, respectively. We analyzed simulations for system sizes $N = 400, 800, 2000$ at a number density $\rho = 1.655$ obtained from previous molecular dynamics simulations [2].

Table 3: Number of analyzed configurations for the tetrahedral network liquid. The number in parenthesis indicates the corresponding number of true stationary points obtained.

–	$T = 0.2900$	$T = 0.3100$	$T = 0.3397$	$T = 0.3716$	$T = 0.4120$
$N = 400$	1200(0.1%)	1200(0.0%)	1200(0.0%)	1200(0.0%)	400(0.0%)
$N = 800$	1200(0.0%)	1200(0.0%)	1200(0.0%)	1200(0.0%)	400(0.0%)
$N = 2000$	800(0.0%)	800(0.0%)	800(0.0%)	799(0.0%)	395(0.0%)

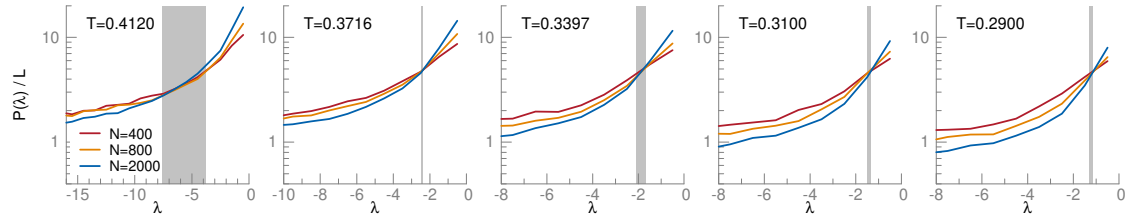

Figure 15: Averaged scaled participation ratio as a function of eigenvalue λ for the tetrahedral network liquid. Vertical arrows mark the mobility edge λ_e at a given temperature. The width of the vertical bar is representative of the uncertainty on λ_e.

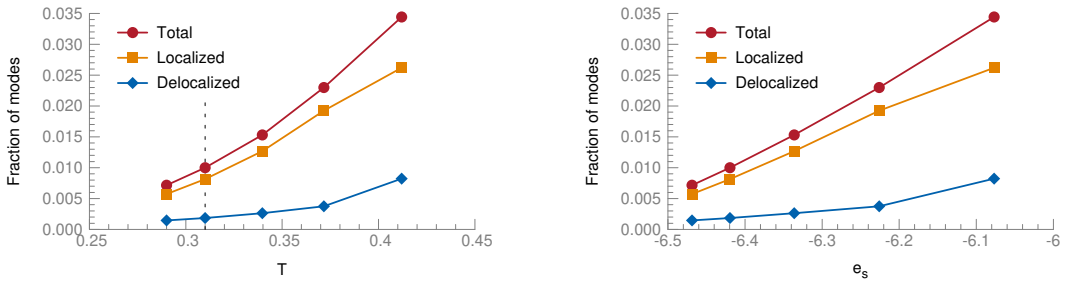

Figure 16: Fraction of unstable modes as a function of (a) temperature and (b) energy for the tetrahedral network liquid ($N = 2000$). The vertical arrow in panel (a) marks the mode-coupling temperature T_{MCT}

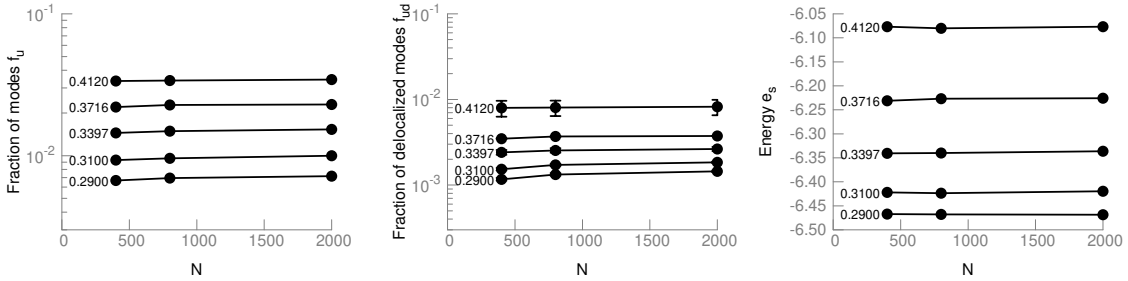

Figure 17: (a) Fraction of unstable modes, (b) fraction of delocalized unstable modes and (c) energy of stationary points as a function of the number of particles N for the tetrahedral network liquid

3.5 Polydisperse particles n=18

We consider the model of polydisperse repulsive particles with additive interactions studied in Ref. [10]. The interaction potential between particles i and j is

$$u(r_{ij}) = \epsilon(\sigma_{ij}/r_{ij})^n + c_4\left(\frac{r_{ij}}{\sigma_{ij}}\right)^4 + c_2\left(\frac{r_{ij}}{\sigma_{ij}}\right)^2 + c_0 \tag{6}$$

with $n = 18$ and $\sigma_{ij} = (\sigma_i+\sigma_j)/2$. The coefficients c_0, c_2, c_4 are determined to ensure continuity of the potential at the cut-off distance $r_{cut} = 1.25\sigma_{ij}$, as for the ternari mixture. The distribution of particle diameters is $P(\sigma) = A/\sigma^3$ for $\sigma_{max} \leq \sigma \leq \sigma_{min}$ and 0 otherwise, with A a normalization constant. We use $\sigma_{max}/\sigma_{min} = 2.219$, which implies a root mean square deviation of the diameter

$$\delta = \frac{\sqrt{\langle\sigma^2\rangle - \langle\sigma\rangle^2}}{\langle\sigma\rangle}, \tag{7}$$

of about 23%. We simulated systems composed of $N = 500, 1000, 1500$ particles at a number density $\rho = 1$ using the swap Monte Carlo algorithm described in Ref. [10].

Table 4: Number of analyzed configurations for the polydisperse soft spheres with $n = 18$. The number in parenthesis indicates the corresponding number of true stationary points obtained.

–	$T = 0.330$	$T = 0.350$	$T = 0.390$	$T = 0.432$	$T = 0.471$	$T = 0.517$	$T = 0.586$	$T = 0.68$
$N = 250$	1001(52.7%)	1001(39.4%)	1001(24.0%)	1001(14.0%)	1001(7.2%)	1001(5.4%)	1001(3.3%)	1001(3.6
$N = 500$	1001(26.2%)	1001(15.6%)	1001(6.3%)	1001(1.4%)	1001(0.6%)	1001(0.7%)	1001(0.5%)	1001(0.3
$N = 1500$	459(2.0%)	400(0.2%)	400(0.0%)	400(0.0%)	400(0.0%)	400(0.0%)	400(0.0%)	400(0.0%

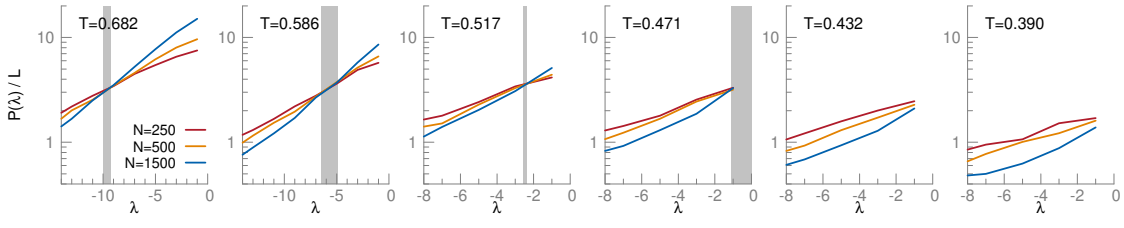

Figure 18: Averaged scaled participation ratio as a function of eigenvalue λ for polydisperse soft spheres with $n = 18$. Vertical arrows mark the mobility edge λ_e at a given temperature. The width of the vertical bar is representative of the uncertainty on λ_e.

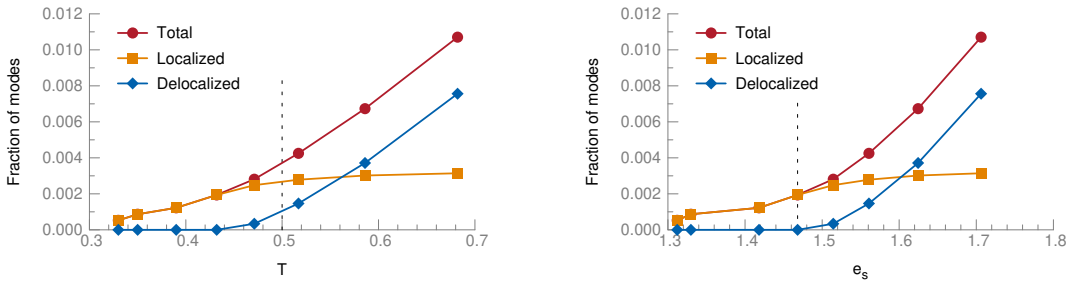

Figure 19: Fraction of unstable modes as a function of (a) temperature and (b) energy for the polydisperse soft spheres with $n = 18$ ($N = 1500$). Vertical arrows in panel (a) and (b) mark the mode-coupling temperature T_{MCT} and the threshold energy e_{th}, respectively.

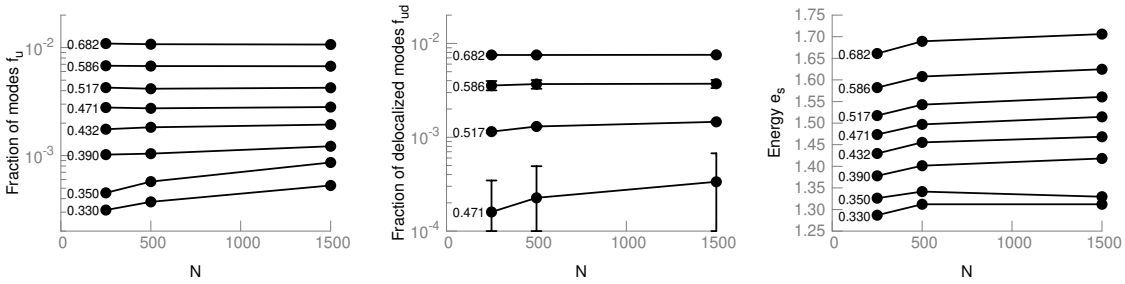

Figure 20: (a) Fraction of unstable modes, (b) fraction of delocalized unstable modes and (c) energy of stationary points as a function of the number of particles N for the polydisperse soft spheres with $n = 18$

3.6 Polydisperse particles n=12

This is a variant of the polydisperse mixture introduced in the previous section. It features non-additive interactions to stabilize the fluid against phase separation [10]. The interaction potential between particles i and j is

$$u(r_{ij}) = \epsilon(\sigma_{ij}/r_{ij})^n + c_4\left(\frac{r_{ij}}{\sigma_{ij}}\right)^4 + c_2\left(\frac{r_{ij}}{\sigma_{ij}}\right)^2 + c_0 \tag{8}$$

with $n = 12$ and $\sigma_{ij} = (1-0.2|\sigma_i-\sigma_j|)(\sigma_i+\sigma_j)/2$. The coefficients c_0, c_2, c_4 are determined to ensure continuity of the potential at the cut-off distance $r_{cut} = 1.25\sigma_{ij}$. We use $\sigma_{max}/\sigma_{min} = 2.219$ which implies $\delta \approx 23\%$. We simulated systems composed of $N = 500, 1000, 1500$ particles at a number density $\rho = 1$ using the swap Monte Carlo algorithm described in Ref. [10].

Table 5: Number of analyzed configurations for the polydisperse soft spheres with $n = 12$. The number in parenthesis indicates the corresponding number of true stationary points obtained.

–	$T = 0.062$	$T = 0.075$	$T = 0.092$	$T = 0.110$	$T = 0.120$	$T = 0.150$
$N = 250$	1000(19.1%)	1000(5.5%)	1000(0.5%)	1000(0.2%)	1000(0.1%)	1000(0.2%)
$N = 500$	1000(5.0%)	1000(0.5%)	1000(0.0%)	1000(0.0%)	1000(0.0%)	1000(0.0%)
$N = 1500$	400(0.0%)	400(0.0%)	400(0.0%)	400(0.0%)	400(0.0%)	400(0.0%)

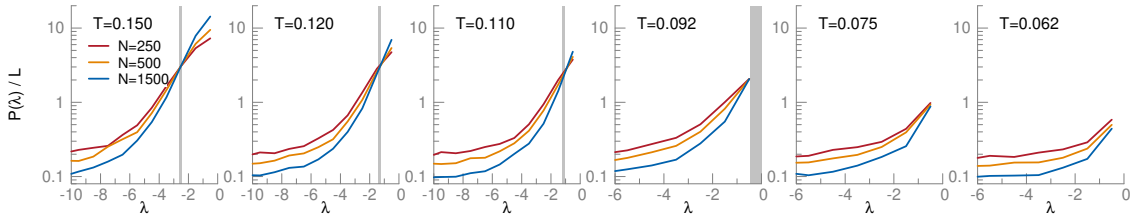

Figure 21: Averaged scaled participation ratio as a function of eigenvalue λ for the polydisperse soft spheres with $n = 12$. Vertical arrows mark the mobility edge λ_e at a given temperature. The width of the vertical bar is representative of the uncertainty on λ_e.

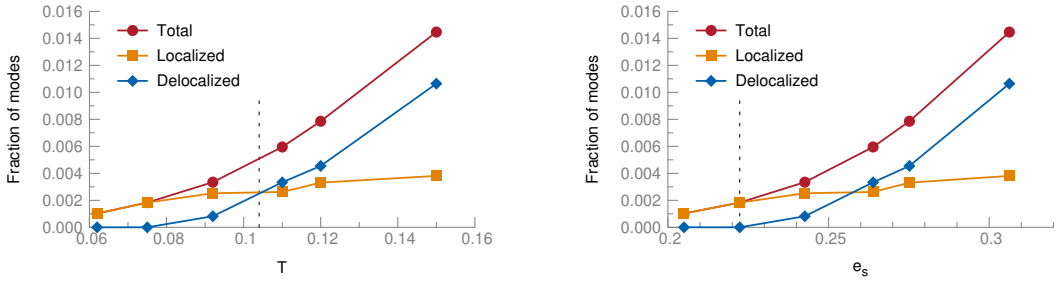

Figure 22: Fraction of unstable modes as a function of (a) temperature and (b) energy for the polydisperse soft spheres with $n = 12$ (N=1500). Vertical arrows in panel (a) and (b) mark the mode-coupling temperature T_{MCT} and the threshold energy e_{th}, respectively.

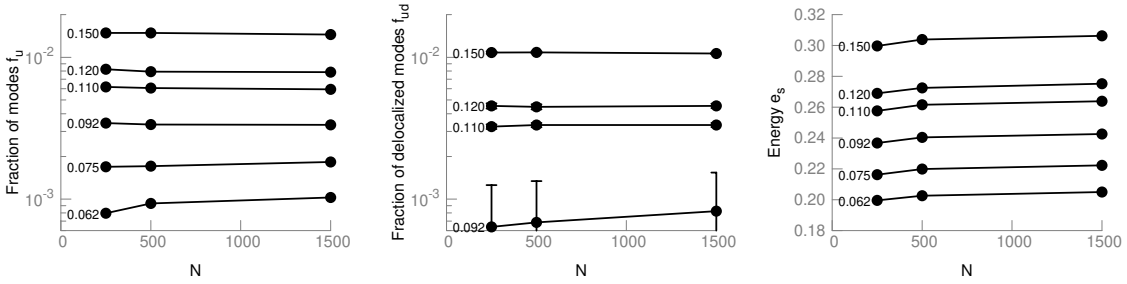

Figure 23: (a) Fraction of unstable modes, (b) fraction of delocalized unstable modes and (c) energy of stationary points as a function of the number of particles N for the polydisperse soft spheres with $n = 12$

References

[1] B. Bernu, J. P. Hansen, Y. Hiwatari, and G. Pastore. Soft-sphere model for the glass transition in binary alloys: Pair structure and self-diffusion. *Phys. Rev. A*, 36:4891, 1987.

[2] Ludovic Berthier, Giulio Biroli, Daniele Coslovich, Walter Kob, and Cristina Toninelli. Finite-size effects in the dynamics of glass-forming liquids. *Phys. Rev. E*, 86(3), 2012.

[3] D. Coslovich and G. Pastore. Dynamics and energy landscape in a tetrahedral network glass-former: Direct comparison with models of fragile liquids. *J. Phys. Condens. Matter*, 21:285107, 2009.

[4] Jonathan P. K. Doye and David J. Wales. Comment on "Quasisaddles as relevant points of the potential energy surface in the dynamics of supercooled liquids" [J. Chem. Phys. 116, 10297 (2002)]. *J. Chem. Phys.*, 118:5263, 2003.

[5] Tomàs S. Grigera, Andrea Cavagna, Irene Giardina, and Giorgio Parisi. Geometric Approach to the Dynamic Glass Transition. *Phys. Rev. Lett.*, 88:055502, 2002.

[6] Tomás S. Grigera and Giorgio Parisi. Fast Monte Carlo algorithm for supercooled soft spheres. *Phys. Rev. E*, 63:045102, 2001.

[7] R. Gutiérrez, S. Karmakar, Y. G. Pollack, and I. Procaccia. The static lengthscale characterizing the glass transition at lower temperatures. *EPL*, 111:56009, 2015.

[8] Smarajit Karmakar, Edan Lerner, Itamar Procaccia, and Jacques Zylberg. Effect of the interparticle potential on the yield stress of amorphous solids. *Phys. Rev. E*, 83:046106, 2011.

[9] D. C. Liu and J. Nocedal. *Math. Program.*, 45:503, 1989.

[10] Andrea Ninarello, Ludovic Berthier, and Daniele Coslovich. Models and Algorithms for the Next Generation of Glass Transition Studies. *Phys. Rev. X*, 7:021039, 2017.

[11] M Sampoli, P Benassi, R Eramo, L Angelani, and G Ruocco. The potential energy landscape in the Lennard-Jones binary mixture model. *J. Phys. Condens. Matter*, 15:S1227–S1236, 2003.